Magnetism and local order: *Ab initio* tight-binding theory

Feng Liu, M. R. Press, S. N. Khanna, and P. Jena
Physics Department, Virginia Commonwealth University, Richmond, Virginia 23284-2000
(Received 6 September 1988)

The effects of the local environment on the electronic structure and magnetic moments of Fe, Co, and Ni have been studied by confining these atoms to assume various structural forms such as chains, surfaces, layers, and crystals. The coordination number of the atoms can thus be changed over a wide range. The local environment of the magnetic atom has also been altered by introducing defects such as impurities, vacancies, and vacancy complexes. A simple method based upon the real space was devised that enables us to calculate the electronic structure of perfect as well as imperfect systems with speed and accuracy. The method is based upon a cross between the molecular-cluster and the tight-binding theories and contains *no* adjustable parameters. The effect on the magnetic moments due to vacancies, vacancy clusters, and surface relaxations in Fe are studied to illustrate the versatility of the method. The results in chains, slabs, and bulk are compared with earlier theoretical results, as well as available experimental data. The excellent agreement achieved in these comparisons provides room for optimism that our theory can be useful in studying complex systems otherwise inaccessible to modern-day theories.

I. INTRODUCTION

With the advent of sophisticated experimental tools for preparing and characterizing exotic materials and the development of highly accurate theoretical methods for understanding their fundamental properties, material science is taking on a new look. Interest is now growing in the design and fabrication of materials not found in nature that can suit one's specifications. This new era of atomic engineering involves superlattices, modulated structures, over-layers, and cluster materials. The properties of these materials, which have atomic dimensions, can be as varied as their structure and composition. Applications of these materials in the electronic, magnetic, energy, and optical industries are among a few that show promise for the near future.

These materials are also providing a real challenge to theorists to unravel the mysteries concerning the unusual size and structural dependence of their electronic properties. In spite of the inherent difficult in a fundamental theoretical understanding due to the reduced symmetry and dimensionality of these systems, notable progress has been made during the last decade—thanks to the development of the density-functional theory and high-speed computers. Among the *ab initio* theories, the most widely used ones are (i) the full-potential linearized augmented-plane-wave (FLAPW) method,[1] (ii) the linearized muffin-tin-orbital (LMTO) method,[2] and (iii) the self-consistent-field–linear combination of atomic orbitals–molecular-orbital (SCF-LCAO-MO) method.[3] The FLAPW method can yield quantitatively accurate total energies and all properties that can be derived from it. It has been used successfully to calculate the electronic structure and magnetic properties of bulk, surfaces, thin films, and modulated structures. Since the method inherently makes use of the Bloch's theorem, it is best suited for studying systems with long-range periodic order. Study of imperfections is still possible[4] within the FLAPW framework if one assumes the lattice to consist of a periodic repetition of supercells comprising the defect site and a few of its surrounding host atoms. The disadvantage of this approach is that computational limitations restrict the size of the supercell, giving rise to an undesirably large defect concentration. While this can be avoided in the LMTO method due to the use of the host Green's function, the total energies are still difficult to calculate. The SCF-LCAO-MO method[3] based upon the density-functional theory or more sophisticated quantum chemical procedures[5] is a real-space-based technique and can be applied to perfect as well as imperfect systems with equal ease. The method, however, relies on the assumption that the local environment dominates the calculation of all the electronic properties. Thus, one approximates the system by a cluster of atoms which can then be embedded in the host to simulate the lattice. The difficulty with this technique is that one is usually limited to about 40 atoms in a cluster. Thus, "Is the cluster big enough?" remains a nagging question with no satisfactory answer. In addition, all these techniques are very computer intensive and many problems, such as complex defects on surfaces or in bulk, cannot be treated even on the world's fastest computer.

There are, however, semiempirical and approximate methods that can be used to study complex systems involving low symmetry and dimension. Among these, tight-binding[6] and effective-medium based theories[7] are most widely used by the theorists. The tight-binding method, designed for localized or quasilocalized bands, involves parameters that are conventionally determined from bulk band-structure data. However, the transferability of these parameters to systems with reduced symmetry and dimensionality has been in doubt. Recent

studies[8] show that tight-binding parameters obtained from bulk Fe data cannot explain the band structure of Fe in linear chain. This problem is similar to the use of interatomic potentials obtained from bulk data to interpret structural evolution in small finite systems, such as clusters. Here again one finds[9] that the structures of small clusters obtained from bulk-derived interatomic potentials are at variance with the *ab initio* results.[10]

In our laboratory, we have initiated a theoretical program for studying the electronic structure and properties of finite systems with reduced symmetry and dimensionality, such as small homo- and heteroatomic clusters, surfaces with and without imperfections, thin films, vacancies and vacancy clusters in bulk materials, and vacancy-impurity complexes in transition metals. Recently, we have illustrated[11] that interatomic potentials obtained from self-consistent total-energy calculations of Be dimers, trimers, and tetramers can successfully explain the evolution of the structural and electronic properties not only in larger clusters but also in the bulk.

Here we present a method for the transition-metal elements. It is based upon a cross between the molecular cluster and the tight-binding method. We determine, from first principles, the various overlap matrix elements[12] ($dd\sigma$, $dd\pi$, $dd\delta$, $sd\sigma$, and $ss\sigma$) appearing in a tight-binding formulation from the self-consistent treatment of the dimer. Here the two atoms are placed at their corresponding bulk distance. The moment approach[13] is then used to calculate the electron spin density of states and magnetic moments of ferromagnetic transition-metal elements. We refer to this method as the *ab initio* tight-binding (ATB) method, since all the tight-binding parameters used here are calculated from the *ab initio* SCF-LCAO-MO theory.

This method is applied to study the magnetic moments of Fe, Co, and Ni in linear chains, thin slabs consisting of 1, 3, 5, 7, and 9 layers with different crystallographic directions and bulk. To demonstrate the versatility of this method, we have also applied it to study the effects of vacancies, vacancy clusters, and surface relaxation on the magnetic moment of bulk and (100) surface of Fe.

Our emphasis on studying the magnetic moments is due to the long-standing controversy in this field[14] and due to the vast amount of other available theoretical calculations[15] that our results can be compared with. The magnetism of surfaces in modulated structures is also a fascinating problem. While there is no conclusive experimental evidence for surface magnetism, current theories[15,16] predict enhancements of surface magnetism. We show here that our simple approach can yield magnetic moments in very good agreement with other state-of-the-art calculations.[15,16] Furthermore, we illustrate that the tight-binding parameters derived here are transferable to different environments. The fact that our method is not computer intensive (calculation of a 20 000-atom cluster in IBM 3081D computer requires only 20 min of CPU time) means that we can study more complex systems faster.

In the next section we provide a brief outline of our procedure. In Sec. III we present our results for Fe, Co, and Ni. The paper is summarized in Sec. IV.

II. THEORETICAL METHOD

We discuss our approach in two steps. First we recall the main features of the molecular-cluster calculations based on the discrete-variation method (DVM).[17] We then outline the moment approach[13] and show how it can be put on an *ab initio* basis when combined with DVM.

Consider a system of N particles described by a one-electron Hamiltonian, H, in atomic units,

$$H=-\tfrac{1}{2}\nabla^2+\int d\mathbf{r}'\frac{\rho(\mathbf{r}')}{|\mathbf{r}'-\mathbf{r}|}+\sum_j\frac{Z_j}{|\mathbf{r}-\mathbf{R}_j|}+V_{xC}^{\sigma}(\mathbf{r})\ . \quad (1)$$

Here j is the atomic site index. The second and the third terms represent, respectively, the electronic and nuclear contribution to the electrostatic energy. The last term is the exchange-correlation contribution to the potential for spin σ and is approximated by the von Barth–Hedin approximation[18] to the local-spin-density (LSD) functional. The wave function ψ for the system is expressed in terms of a linear combination of atomic orbitals (LCAO) $|i,\lambda\rangle$ localized at site i. λ represents the spin-orbital index

$$\psi=\sum_{i,\lambda}C_{i\lambda}\phi_{i\lambda}\ . \quad (2)$$

We assume that $\phi_{i\lambda}=|i,\lambda\rangle$ form a complete orthonormal set (the orthogonality condition can be easily relaxed). The C_i are variational parameters to be determined from a solution of the Rayleigh-Ritz equation,

$$(\underline{H}-E\underline{S})\underline{C}=0\ , \quad (3)$$

where $\underline{H}$ and $\underline{S}$ are the Hamiltonian and overlap matrices and E is the eigenvalue. In the DVM the Hamiltonian and the overlap matrix element are evaluated as weighted sums over a set of points r_k with weight functions $w(r_k)$, namely,[17]

$$H_{ij}^{\lambda\mu}=\langle i,\lambda|H|j,\mu\rangle=\sum_{r_k}w(r_k)\phi_{i\lambda}^{*}(r_k)H\phi_{j\mu}(r_k)\ , \quad (4)$$

$$S_{ij}^{\lambda\mu}=\langle i,\lambda|j,\mu\rangle=\sum_{r_k}w(r_k)\phi_{i\lambda}^{*}(r_k)\phi_{j\mu}(r_k)\ . \quad (5)$$

In actual LCAO calculations one starts with a set of atomic orbitals $|i,\lambda\rangle$ corresponding to a given atomic configuration and calculates the Hamiltonian matrix elements. Starting from a set of C_i corresponding to atomic orbitals $|i,\lambda\rangle$, the Hamiltonian matrix elements are used to construct the Hamiltonian and overlap matrices. The matrix $(\underline{H}-E\underline{S})$ is then diagonalized to determine a new set of C_j and the process repeated until self-consistency is achieved. Since the size of the matrix depends on the number of atoms and the number of orbitals per atom, the computational time increases rapidly with size (N^3–N^5 depending on the details of the theoretical scheme) and one is restricted to systems having at most a few dozen atoms.

It is clear that if one wants to treat systems having several thousand atoms, one has to go to a different scheme. It is important to realize that the diagonalization of the Hamiltonian equation provides us with the

eigenstates of the whole system. On the other hand, the quantity of prime interest is the local electronic density of states $n_i(E)$. They are related[13] to the resolvant, $R(Z)$,

$$R(Z)=\frac{1}{Z-H} \tag{6}$$

by the equality

$$n_i(E)=\frac{-1}{\pi}\lim_{\varepsilon\to 0}\mathrm{Im}R_i(E+i\varepsilon)\ . \tag{7}$$

As was first shown by Cyrot,[13] the coefficients in the power expansion of $\langle i,\lambda|R(Z)|i,\lambda\rangle$ are nothing but the moments $\mu_n^{i,\lambda}$ of the local density of states n_i. They can be expressed as

$$\begin{aligned}\mu_n^{i,\lambda}&=\langle i,\lambda|H^n|i,\lambda\rangle\\&=\sum_{\substack{j,k,\cdots\\ \mu,\lambda,}}\langle i,\lambda|H|j,\mu\rangle\langle j,\mu|H|k,\nu\rangle\\&\quad\times\langle k,\nu|H\cdots H|i,\lambda\rangle\ ,\end{aligned} \tag{8}$$

with

$$R_i^{\lambda}(Z)=\sum_{p=0}^{\infty}\frac{\mu_p^{i,\lambda}}{Z^{p+1}}\ . \tag{9}$$

Knowing the moments one can calculate $R(Z)$ and hence $n_i(E)$. The actual passage from μ_n to $n_i(E)$ proceeds via a continued fraction[19] for $G(Z)$ given by

$$G(Z)=\cfrac{1}{Z-a_1-\cfrac{b_1}{Z-a_2-\cfrac{b_2}{\ddots}}}\ . \tag{10}$$

The coefficients a_n and b_n are related to moments up to order $(2n+1)$. It is easy to show that coefficients of increasing n include contributions from more and more distant regions, and in most cases one can obtain a reasonable $n_i(E)$ from only a few moments. This is due to the fact that local electronic structure is primarily dominated by the local surroundings. Contrary to the previous case where one diagonalizes H, the present approach requires a calculation of $\mu_n^{i,\lambda}$ which are sums over closed loops of n steps starting from the site i and are extremely easy to calculate numerically.

We combine the LCAO and the moment approach to prescribe a new *ab initio* tight-binding (ATB) method. The matrix elements $\langle i,\lambda|H|j,\mu\rangle$ appearing in Eq. (8) are calculated from the self-consistent solution of the dimer (with bond length confined to the bulk interatomic distance) within the local-spin-density approximation and the discrete variational method.[17] Here the Hamiltonian H is determined self-consistently while the orbitals $|i,\lambda\rangle$ are our starting atomic orbitals. With this formulation we avoid the common practice[20] of fitting the matrix elements to existing bulk band structure. Thus, the present method not only has the advantage that all parameters entering into our theory are calculated from first principles, but, as will be shown later, they are transferable to systems with finite size as well as with reduced symmetry.

This method can also be made into a fully self-consistent moment scheme in the following manner. One would start with atomic orbitals $|i,\lambda\rangle$ corresponding to a given atomic configuration, calculate the Hamiltonian matrix elements $\langle i,\lambda|H|j,\mu\rangle$, and use them in the moment expansion to calculate $n_i(E)$ from which one can calculate occupation of various states by integrating up to the Fermi energy. The new occupation numbers can be used to generate a new set of orbitals $|i,\lambda\rangle$ and iterate until self-consistency. Such a procedure is under way.

III. RESULTS

By carrying out a spin-polarized *ab initio* LCAO-MO calculation of dimer we obtained two sets of Slater-Koster parameters[12] for spin-up and spin-down electrons separately. We then apply them to the moment method one by one to derive density of states for both majority-spin band and minority-spin band. The band splitting can be easily subtracted from the mean of spin-up and spin-down diagonal matrix elements in the dimer calculation. Thus, the magnetic properties can be evaluated by using this new tight-binding approach. The magnetic moments in Fe, Co, and Ni are calculated by using the $4s$ and $3d$ orbitals and the continued fraction constructed from 22 moments. The densities of states for spin-up and -down electrons were obtained by averaging over the partial orbital density of states in the following manner:

$$n_i(E)=\frac{1}{M}\sum_{\alpha=1}^{M}n_i^{\alpha}(E)\ , \tag{11}$$

where M is the number of orbitals.

In Table I we have compared the tight-binding parameters obtained in this work with those obtained by various other groups. One notices large variations in parameters indicating a need for their *ab initio* determination.

In Tables II–IV we present the Slater-Koster parameters ($ss\sigma$, $sd\sigma$, $dd\sigma$, $dd\pi$, and $dd\delta$) for Fe, Co, and Ni, respectively, as calculated using the SCF-LCAO-MO DVM. The bond lengths of the dimers were chosen to be equal to their interatomic separation in the bulk. For Fe

TABLE I. Comparison of tight-binding parameters for Fe obtained by various groups.

Reference	$dd\sigma$	$dd\pi$	$dd\delta$
Present	−0.0557	0.0501	−0.0121
a	−0.0495	0.0267	0
b	−0.0490	0.0300	−0.0028
c	−0.0715	0.0338	−0.0044
d	−0.0538	0.0377	−0.0044
e	−0.0547	0.0359	−0.0080
f	−0.0624	0.0427	−0.0090

[a]W. A. Harrison, in Ref. 6.
[b]Reference 20.
[c]M. C. Desjonqueres and F. Cyrot-Lackmann, J. Phys. F **5**, 1368 (1975).
[d]R. A. Deegan, Phys. Rev. **171**, 659 (1968).
[e]J. F. Cornwell, D. M. Hum, and K. G. Wong, Phys. Lett. **26A**, 365 (1968).
[f]Y. Boudeville, J. Rouseseau-Voilet, F. Cyrot-Lackmann, and S. N. Khanna, J. Phys. (Paris) **44**, 433 (1983).

TABLE II. Slater-Koster parameters for Fe (a) at first NN distance and (b) at second NN distance.

	Spin-up	Spin-down
	(a)	
$ss\sigma$	−0.2122	−0.1938
$sd\sigma$	−0.0592	−0.0580
$dd\sigma$	−0.0557	−0.0556
$dd\pi$	0.0515	0.0487
$dd\delta$	−0.0125	−0.0117
	d-band splitting, $\Delta=\lvert\varepsilon_d^{\uparrow}-\varepsilon_d^{\downarrow}\rvert=0.2$ (Ry)	
	(b)	
$ss\sigma$	−0.1655	−0.1513
$sd\sigma$	−0.0524	−0.0500
$dd\sigma$	−0.0352	−0.0343
$dd\pi$	0.0281	0.0263
$dd\delta$	−0.0058	−0.0053

TABLE III. Slater-Koster parameters for Co.

	Spin-up	Spin-down
$ss\sigma$	−0.2290	−0.2159
$sd\sigma$	−0.0606	−0.0594
$dd\sigma$	−0.0490	−0.0482
$dd\pi$	0.0376	0.0365
$dd\delta$	−0.0081	−0.0078
	d-band splitting, $\Delta=\lvert\varepsilon_d^{\uparrow}-\varepsilon_d^{\downarrow}\rvert=0.17$ (Ry)	

TABLE IV. Slater-Koster parameters for Ni.

	Spin-up	Spin-down
$ss\sigma$	−0.2131	−0.2090
$sd\sigma$	−0.0576	−0.0563
$dd\sigma$	−0.0470	−0.0461
$dd\pi$	0.0400	0.0394
$dd\delta$	−0.0099	−0.0098
	d-band splitting, $\Delta=\lvert\varepsilon_d^{\uparrow}-\varepsilon_d^{\downarrow}\rvert=0.06$ (Ry)	

TABLE V. Exponent Q for the variation of tight-binding parameters with distance.

	$ss\sigma$	$sd\sigma$	$dd\sigma$	$dd\pi$	$dd\delta$
Fe	1.87	1.28	3.08	4.08	5.07
Co	2.08	1.89	3.75	4.43	4.49
Ni	2.01	1.71	3.34	4.04	4.98

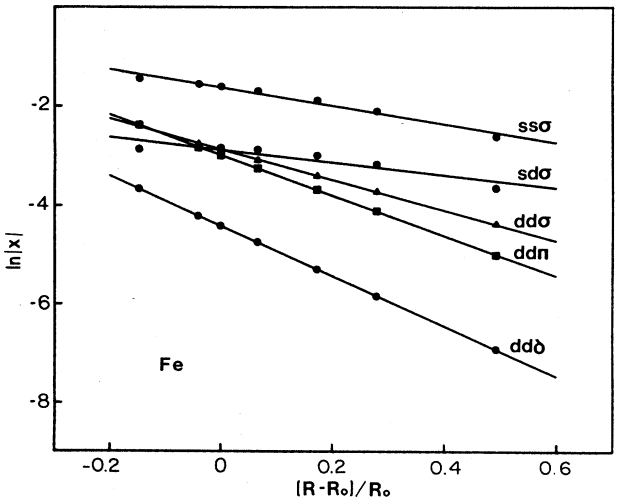

FIG. 1. Variation of tight-binding parameters $ss\sigma$, $sd\sigma$, $dd\sigma$, $dd\pi$, and $dd\delta$ as a function of distance in Fe. x denotes the parameters and $\ln|x|$ is shown as a function of $(R-R_0)/R_0$ with R_0 as the bulk nearest-neighbor separation.

we have presented the parameters for the two nearest neighbors since in the bcc lattice these are not too far apart and the overlap at the second-nearest neighbor, as seen in Table I, can be significant.

For studies of electronic and magnetic behavior under pressure or in situations where interatomic distances change due to relaxations such as at surfaces or around defects in bulk, one requires the above parameters as a function of interparticle spacing. We present in Figs. 1–3 the variation of these parameters with distance for Fe, Co, and Ni, respectively. We have plotted $\ln(x)$ $(x=dd\sigma, dd\pi, \ldots)$ as a function of $(R-R_0)/R_0$ where R_0 is the interparticle distance in the bulk. It is interesting to note that the variation is linear indicating that pa-

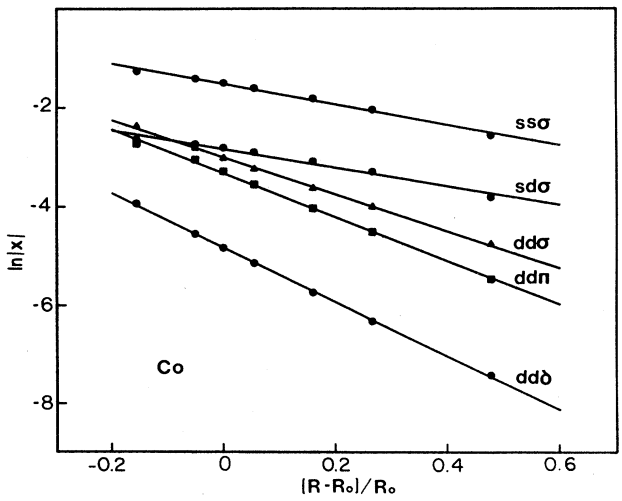

FIG. 2. Variation of tight-binding parameters $ss\sigma$, $sd\sigma$, $dd\sigma$, $dd\pi$, and $dd\delta$ as a function of distance in Co. x denotes the parameters and $\ln|x|$ is shown as a function of $(R-R_0)/R_0$ with R_0 as the bulk nearest-neighbor separation.

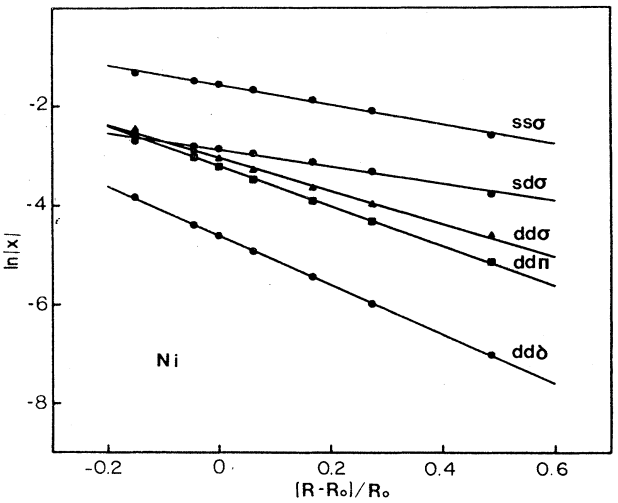

FIG. 3. Variation of tight-binding parameters $ss\sigma$, $sd\sigma$, $dd\sigma$, $dd\pi$, and $dd\delta$ as a function of distance in Ni. x denotes the parameters and $\ln|x|$ is shown as a function of $(R-R_0)/R_0$ with R_0 as the bulk nearest-neighbor distance.

rameters vary exponentially with distance. In Table V we give the exponents (Q) corresponding to

$$x = x_0 \exp[-Q(R-R_0)/R_0] , \tag{12}$$

fitted using R values from 4 to 7 a.u. In Fig. 4 the variation of the band splitting Δ between spin-up and spin-down as a function of distance is given. The variation is small except for Fe at small distances. Ferromagnetic order was assumed for all of these distances. For Fe we had also calculated the total energy of the dimer by assuming antiferromagnetic coupling. The energies for all of the distances considered here for ferromagnetic order are lower than those for the antiferromagnetic case. Notice that Δ in Ni behaves qualitatively different from that in Co and Fe. The band splitting Δ increases with decreasing distance in Ni while the reverse is true for Fe and Co.

We have used the above parameters to study the variation of electronic structure and magnetic moment for the case of bulk, thin films, and defects in Fe, Co, and Ni.

A. Bulk crystal

In Figs. 5, 6, and 7 we compare the electron spin density of states calculated using the present method with the self-consistent band calculations of Moruzi *et al.*[21] for Fe, Co, and Ni, respectively. It is clear that our results, shown in dashed lines, reproduce all the salient features of the density of states for both spins in all the three elements. These include the location of the Fermi energy in the density of states, the location of the major peaks, and the antibonding states as well as the bandwidth. The lack of fine structure in our density of states (DOS) is simply due to our use of small number of moments (22 in the present case). Many of the fine peaks in the bulk DOS are related to van Hove singularities and require large number of moments. In this work we are primarily concerned with integrated quantities that are well represented by using only 22 moments.

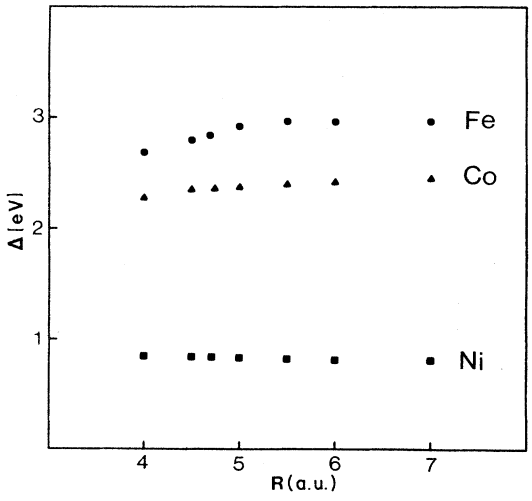

FIG. 4. Band splitting Δ corresponding to separation between diagonal Hamiltonian matrix elements for the up- and down-spin d states as a function of interparticle separation in Fe (circles), Co (triangles), and Ni (squares) diatomic molecules.

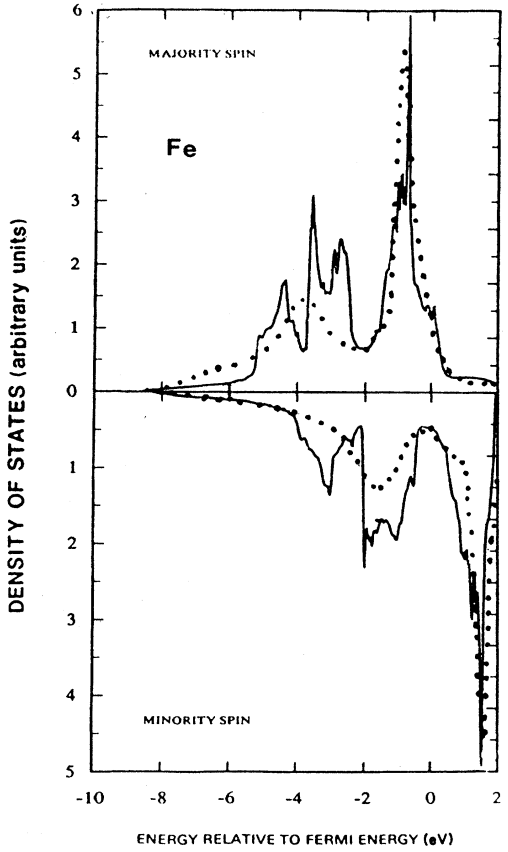

FIG. 5. Density of electronic states in bulk Fe. Dotted lines are our results and the solid lines are taken from Ref. 21. All energies are relative to the Fermi energy.

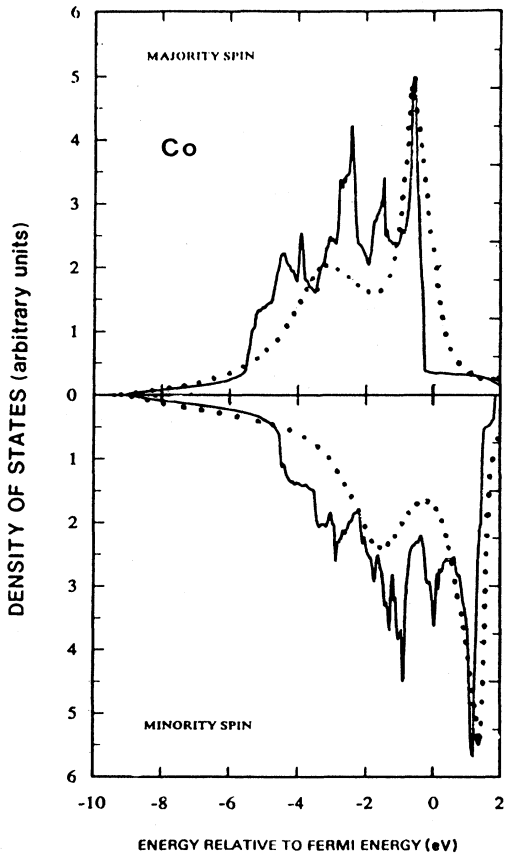

FIG. 6. Density of electronic states in bulk Co. The legend is the same as in Fig. 5.

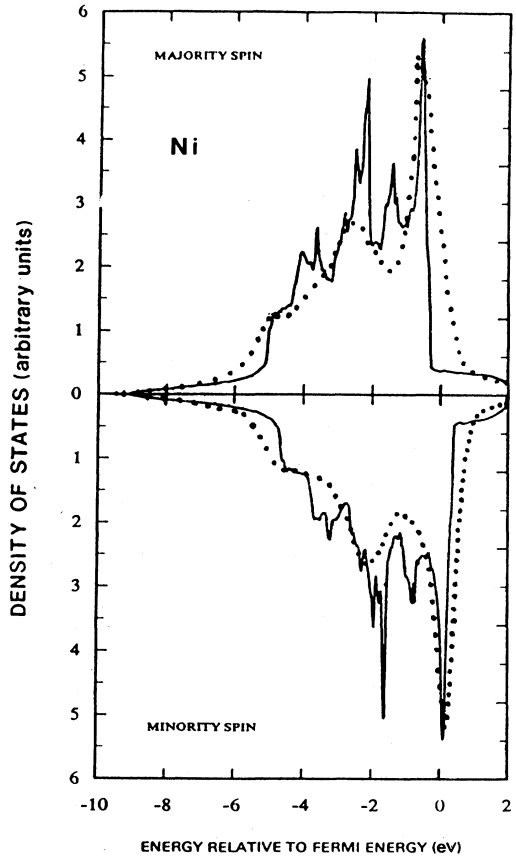

FIG. 7. Density of electronic states in bulk Ni. The legend is the same as in Fig. 5.

In Table VI the bulk magnetic moments of Fe, Co, and Ni computed by integrating the majority and minority spin density of states are given. Note that our results compare quite well with the experimental values as well as the band-structure results.

In Fig. 8 the magnetic moments referenced to their corresponding bulk values are plotted as a function of coordination number in Fe, Co, and Ni. The coordination number (CN) defines the number of nearest-neighbor atoms. For Ni, the coordination numbers of 2, 4, 6, 8, 9, and 12 correspond to linear chain, (100) monolayer, (111) monolayer, (100) surface, (111) surface, and bulk, respectively. Similar for Co, we plot moments for linear chain, (111) monolayer, (111) surface, and bulk representing CN's of 2, 6, 9, and 12. For Fe, CN's of 2, 4, 7, 9, 10, 13, and 14 correspond to linear chain, (100) monolayer, an atom at the inner surfaces of a 51 atom void, 9 atom void,

TABLE VI. Magnetic moments (in units of μ_B) in bulk Fe, Co, and Ni.

	Present method	Band structure	Expt.
Fe	2.53	2.15	2.2
Co	1.69	1.56	1.6
Ni	0.59	0.59	0.6

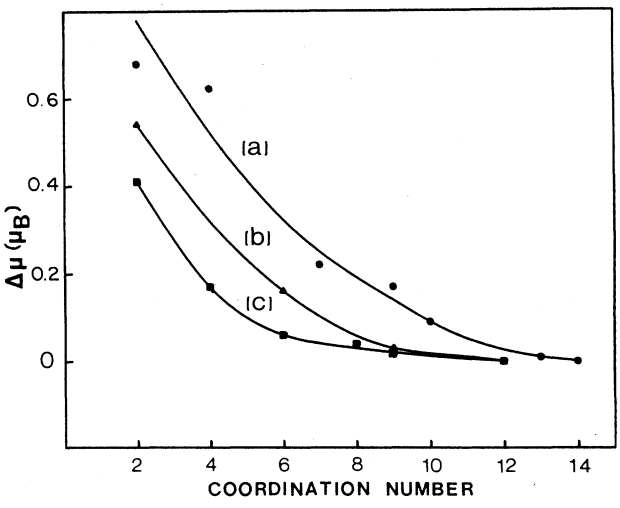

FIG. 8. Deviation from the bulk magnetic moment $\Delta\mu$ in Fe, Co, and Ni as a function of the nearest coordination number (in various structures). (a), (b), and (c) correspond to Fe, Co, and Ni, respectively. The smooth lines are drawn simply to guide the eye.

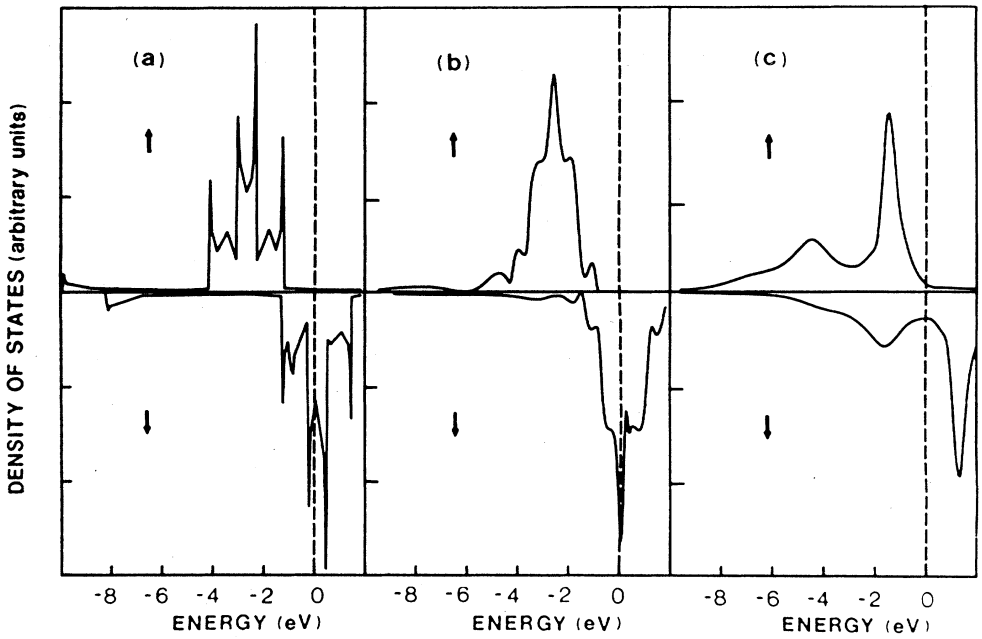

FIG. 9. Density of electronic states for majority and minority spins in (a) linear chain, (b) (100) monolayer, and (c) bulk Fe. The Fermi energy is at $E=0$.

15 atom void, monovacancy and bulk Fe, respectively. Note that for Fe, due to the small difference between the first- and second-nearest-neighbor distance, we count both the neighbors in arriving at the coordination number. In all three cases, the moments decrease monotonically as the coordination numbers increase. Thus, an atom is more magnetic than a cluster which is more magnetic than a crystal.

To understand this trend, we plot the spin density of states for different coordination numbers for Fe, Co, and Ni in Figs. 9–11, respectively. In Figs. 9(a)–9(c) the spin density of states of Fe for the linear chain (CN of 2), (100)

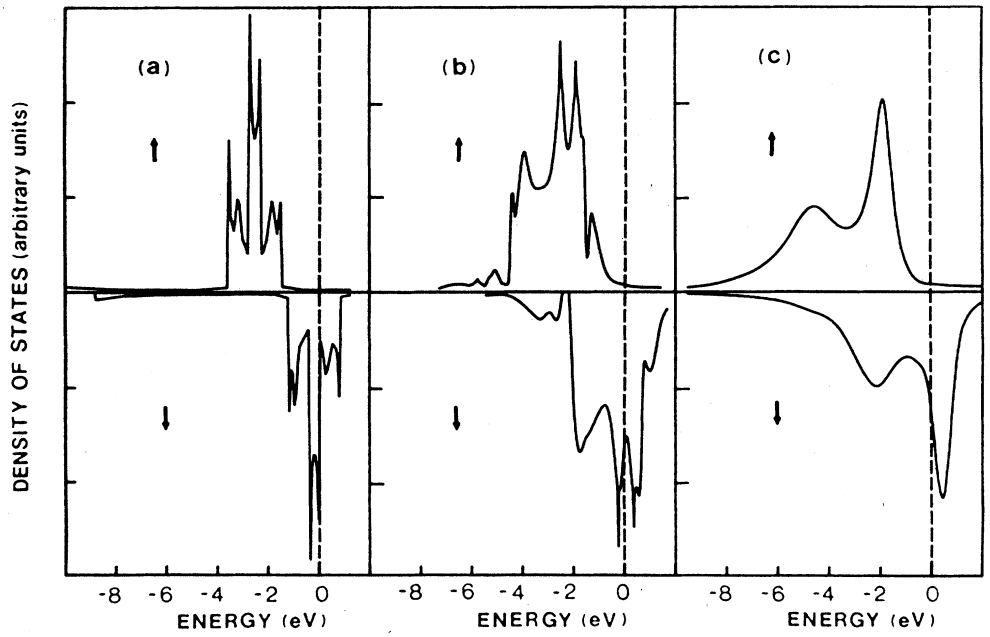

FIG. 10. Density of electronic states for majority and minority spins in (a) linear chain, (b) (001) monolayer, and (c) bulk Co. The Fermi energy is at $E=0$.

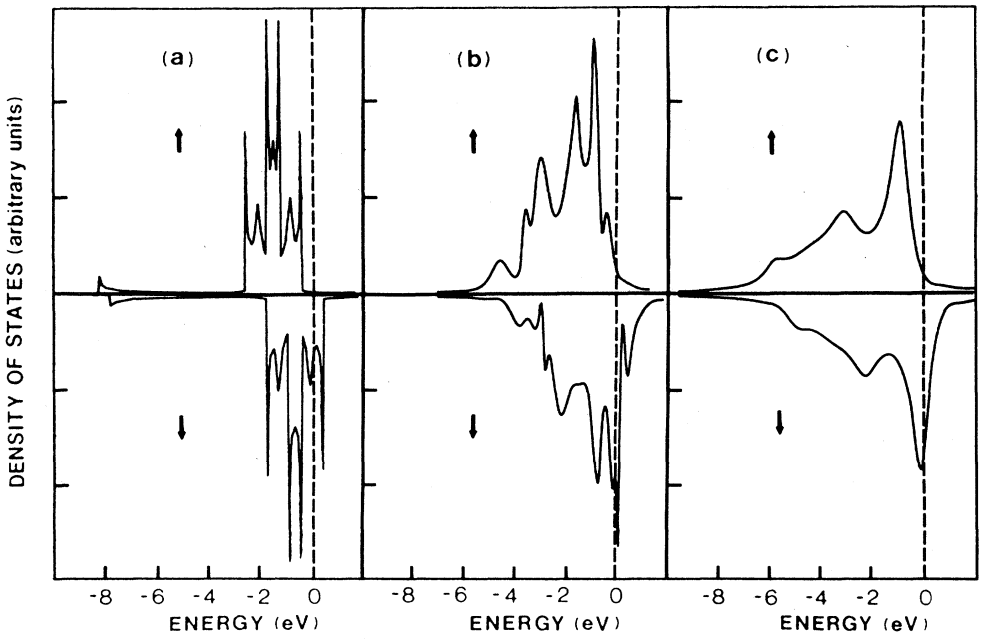

FIG. 11. Density of electronic states for majority and minority spins in (a) linear chain, (b) (111) monolayer, and (c) bulk Ni. The Fermi energy is at $E=0$.

monolayer (CN of 4), and bulk (CN of 14) are plotted. Similarly, the plots in Figs. 10(a)–10(c) correspond, respectively, to coordination numbers of 2, 6, and 12 in Co. Corresponding results are plotted for Ni in Figs. 11(a)–11(c). All these figures have one thing in common: the density of states is narrow in linear chains and broadens as one approaches the bulk. This broadening is caused by the larger overlap between the atomic orbitals as the number of nearest-neighbor atoms increases. As is well known, most atoms have nonzero spins while a few in the solid phase exhibit magnetism. The orbital overlap as atoms form solids is responsible for loss of magnetic character of atoms as they go into a condensed-matter environment.

The reduction in the magnetic moment with increasing coordination is caused, in addition, by a concomitant transfer of electrons from the majority to the minority spin bands as the density of states broadens in going from chains to solids.

The changes in the moments can also be caused by dilating or compressing the lattice. The former would decrease the overlap and hence enhance the moment. The opposite would be the case for compression. It is thus possible to artificially control the magnetic moment by both reducing the coordination number and increasing the interatomic distance at the same time. This procedure can be achieved by adsorbing small clusters (of varying sizes) of Fe, Co, and Ni onto substrates whose intrinsic atomic separations are larger than those found in the elemental magnets. In this case, one also expects the electronic interaction between the cluster and the substrate to play a role in magnetism. We are currently working on this and the results will be published in due course.

Experiments on the magnetic moments of isolated clusters[22] in the gas phase have recently been carried out. One finds[22,23] that the moments, in general, increase with decreasing cluster size. For a proper theoretical understanding one must realize that there are two competing factors that determine the magnetic moments of clusters. The decreasing coordination number in small clusters tends to enhance the moment. On the other hand, the interatomic distances in metallic clusters increase as clusters grow in size. This factor would tend to lower the cluster moments as their size gets smaller. It is for this factor that the moments in small clusters are not as large as they would be otherwise.

B. Chain, thin slabs, and surfaces

We have calculated magnetic moments for linear chains and 1-, 3-, 5-, 7-, and 9-layer slabs of Fe(100), Ni(100), Ni(111), and Co(001) orientations. The results are tabulated in Tables VII–X, and compared with the available band-structure results. We note that our computed magnetic moments for the linear chains are in excellent agreement with the self-consistent FLAPW results

TABLE VII. Magnetic moment per atom in linear chains of Fe, Co, and Ni.

	Present method	FLAPW
Fe	3.21	3.3
Co	2.23	
Ni	1.02	1.1

TABLE VIII. Magnetic moments per atom in 1-, 3-, 5-, 7-, and 9-layer slabs of Fe(100).

	1-layer				7-layer		
	Present	FLAPW	3-layer	5-layer	Present	FLAPW	9-layer
S	3.15	3.20	2.75	2.73	2.74	2.98	2.71
$S-1$			2.56	2.53	2.54	2.35	2.53
$S-2$				2.54	2.55	2.39	2.53
$S-3$					2.55	2.25	2.54
C							2.54

TABLE IX. Magnetic moments per atom in 1-, 3-, 5-, 7-, and 9-layer slabs of Co(001).

	1-layer	3-layer	5-layer	7-layer	9-layer
S	1.85	1.75	1.74	1.74	1.73
$S-1$		1.74	1.71	1.72	1.72
$S-2$			1.71	1.69	1.70
$S-3$				1.70	1.70
C					1.69

TABLE X. Magnetic moments per atom in 1-, 3-, 5-, 7-, and 9-layer slabs of Ni.

Surface Orientation		1-layer Present	1-layer FLAPW	3-layer Present	5-layer Present	5-layer FLAPW (Ref. 15)	5-layer FLAPW (Ref. 16)	7-layer Present	7-layer FLAPW	9-layer Present
(100)	S	0.76	0.86	0.68	0.63	0.61	0.73	0.64	0.68	0.62
	$S-1$			0.56	0.60	0.55	0.68	0.56	0.60	0.54
	$S-2$				0.61	0.58	0.69	0.60	0.59	0.60
	$S-3$							0.61	0.56	0.59
	C									0.57
(111)	S	0.65		0.62	0.61			0.60		0.60
	$S-1$			0.61	0.58			0.58		0.58
	$S-2$				0.58			0.57		0.58
	$S-3$							0.57		0.57
	C									0.58

TABLE XI. Magnetic moments at the inner layer of atoms surrounding the void center in Fe.

Void size (number of vacancies)	Nearest neighbor	Next-nearest neighbor	Coordination number	Moment (μ_B)
Monovacancy	7	6	13	2.55
9	4	5	9	2.70
15	6	4	10	2.61
27	5	5	10	2.64
51	4	3	7	2.75

TABLE XII. Magnetic moments at nearest-neighbor atoms to mono-, di-, tri-, and tetervacancy clusters in Fe(100) 9-layer slabs. Only results for the two top layers are given (see Fig. 12).

	Perfect	1-vacancy Fig. 12(a)	2-vacancy Fig. 12(b)	2-vacancy Fig. 12(c)	3-vacancy Fig. 12(d)	4-vacancy Fig. 12(e)	5% Relaxation
S	2.71	2.73	2.73	2.76	2.73	2.81	2.65
$S-1$	2.53	2.54	2.56	2.56			2.52

of Freeman and co-workers.[15] For Ni(111) and Co(001), the variation in the magnetic moment as one goes from the surface layer (with a coordination number of 9) to the central layer (with a coordination number of 12) in the 9-layer slab is minimal [3% for Ni(111) and 2% for Co(001)]. Here the surfaces are most closely packed and the overlap is already strong even for the surface layer. Thus, changing the coordination number does not play a significant role. On the other hand, for Fe(100) and Ni(100) there is a significant dependence of the magnetic moment on the coordination number. The surface layer magnetism of Fe(100) and Ni(100) is enhanced by 7% and 9%, respectively. In addition, the magnetic moments in Ni(100) exhibit Friedel-like oscillations as one approaches the central layer. The central layer of even the 5-layer slab in all these materials have magnetic moments almost equal to their bulk values, indicating the extent to which surface affects electronic structure in underlying layers. Our results are compared with available FLAPW results. In general, the agreement is gratifying.

C. Point and complex defects

So far we have concentrated on establishing the present method by comparing our results with those available in periodic systems. Now we discuss another aspect: the role of defects on magnetic moments. This is where the strength of our theory is most apparent, since we do not know of any other technique that can compete in a computationally effective manner to treat such a large class of imperfections as discussed below.

We have calculated the magnetic moments at the nearest-neighbor atom to a vacancy in bulk Fe, voids corresponding to the removal of 9, 15, 27, and 51 atoms in Fe (these represent the cumulative number of atoms in the first, second, third, and fourth shells of atoms surrounding the body center), mono-, di-, tri-, and tetravacancy clusters on Fe(100) surface, and an inward relaxation of the surface layer of Fe(100) by 5%. An understanding of the role of defects on magnetic moments is important since very few systems, especially surfaces, are 100% clean.

The magnetic moments at the inner layer of atoms surrounding the void center is given as a function of void size in Table XI. No relaxation of atoms around the void center was considered. Generally, relaxations that decrease the distances between atoms cause the moments to fall. It is interesting to note that these moments also oscillate with void size. In order to understand the source of such an oscillatory behavior, we have given in Table XI the number of nearest- and next-nearest-neighbors of the atoms on the inner shell for various voids. In the case of Fe, the distances of the nearest- and next-nearest-neighbor atoms are close to each other. So we identify the coordination number in Fe as the sum of these two numbers. It is clearly seen that the change in moment is related to the changes in the local environment. Sites having greater coordination numbers show lower moments . Note that for a 51-atom void, the magnetic moment has approached its asymptotic value. No theoretical studies are available to compare with our results in Table XI.

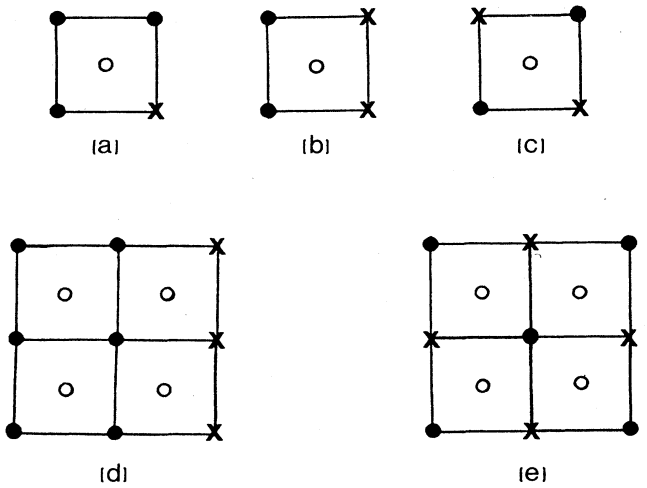

FIG. 12. Geometries of various defects introduced at the surface of Fe(100) 9-layer slab. Solid and open circles define the atom positions on the top two layers. × refers to the vacancy sites. The moments corresponding to these defects are given in Table XII.

In Table XII we present the magnetic moments at the nearest-neighbor atom on the top two layers of the Fe(100) 9-layer slab by introducing mono-, di-, tri-, and tetravacancy clusters on the surface plane. The topologies of these defects are shown in Fig. 12. Note from Table XII that the effect of the vacancy clusters on the magnetic moment, although noticeable, it is not very significant. However, the effect of a surface relaxation on the magnetic moment is much larger—again increasing overlap due to inward relaxation causes the moment to decrease. This exercise demonstrates that a large enhancement of the moment can be achieved by putting "inverse pressure" (and thus increasing interatomic distance) rather than by decreasing the coordination number. An optimum would most likely result if the decrease in coordination number is also combined with an increasing interatomic separation.

IV. CONCLUSIONS

We have developed a theory based upon a combination of the molecular-cluster and tight-binding approaches to calculate the electronic structure and the magnetic moments of transition-metal atoms. A similar approach has been taken by Chadi and Robertson in treating semiconductor systems.[24] Our theory contains no adjustable parameters, is simple and transparent in its construction, computationally efficient, and can be applied to systems containing complex defects just as easily as it can be to systems with perfect periodic order. The theory is applied to determine the density of states and magnetic moments of Fe, Co, and Ni forming linear chains, surfaces, and slabs of varying thickness and crystallographic orientation. The results compare well with the available experimental data and other quantitative theories. The ability of the method to reproduce a wide variety of data in different environmental conditions clearly demon-

strates that the Slater-Koster parameters determined from dimer calculations and used in the tight-binding theory are transferable, much in the same spirit as pseudopotentials determined from atoms are used in clusters to crystals. We have also applied the method to study the effect of imperfections such as vacancies, vacancy clusters, and surface relaxation in Fe. Following is a summary of our important conclusions.

(1) The magnetic moment per atom increases as the number of magnetic atoms in the near-neighbor shell (coordination number) decreases. This is caused by the decrease in the overlap of the nearby atomic orbitals as coordination numbers decrease. This leads to sharper density of states.

(2) The effect of vacancies on the nearest-neighbor magnetic atom tends to enhance its magnetic moment, again due to a decrease in the coordination number.

(3) Surface relaxations that tend to decrease the interlayer separation cause the magnetic moment to decrease due to increasing overlap.

(4) The effect of interatomic distances on the magnetic moment appears to be larger than the coordination number. Thus, it is likely that the moments per atom can be significantly enhanced by depositing monolayers of magnetic elements on substrates whose only role would be to stretch the absorbant's interatomic bond. Calculations are presently underway to investigate these modulated structures.

In spite of the optimism expressed here, the reader should be reminded that the parameters used are determined from diatomic molecules. In situations where many-body terms are important, one might want to go to higher sophistication in the theory. In transition-metal systems, however, the predominant contribution to the magnetic moments comes from the quasilocalized d electrons. The interactions are, therefore, local. This is largely responsible for the success of our present calculation that only uses dimer interactions and neglects higher-body correlation. We expect the three- and more-body terms to be important in less-localized electron systems. We are presently investigating the effect of these terms by recomputing the overlap parameters in larger clusters.

ACKNOWLEDGMENTS

This work was supported in part by a grant from the U.S. Army Research Office (DAAG 29-85-K-0244).

[1]E. Wimmer, H. Krakauer, M. Weinert, and A. J. Freeman, Phys. Rev. B **24**, 864 (1981).

[2]O. K. Anderson, O. Jepsen, and M. Sob, in *Electronic Band Structure and its Applications,* edited by M. Yussouff (Springer-Verlag, Berlin, 1987); H. L. Skriver, *The LMTO Method* (Springer, New York, 1983).

[3]J. C. Slater, *The Self-Consistent Field for Molecules and Solids* (McGraw-Hill, New York, 1974), Vol. 4; D. E. Ellis, in *Handbook on the Physics and Chemistry of Actinides,* edited by A. J. Freeman and G. H. Lander (Elsevier, New York, 1985), p. 1; P. Blaha and J. Callaway, Phys. Rev. B **33**, 1706 (1986); B. K. Rao and P. Jena, J. Phys. F **16**, 461 (1986).

[4]G. P. Kerker, A. Zunger, M. L. Cohen, and M. Schluter, Solid State Commun. **32**, 309 (1979).

[5]W. J. Hehre, L. Radom, P. v.R. Schleyer, and J. A. Pople, *Ab Initio Molecular Orbital Theory* (Wiley, New York, 1986).

[6]W. A. Harrison, *Electronic Structure Properties of Solids* (Freeman, San Francisco, 1980); P. Cyrot-Lackmann and S. N. Khanna, in *Excitations in Disordered Systems,* edited by M. F. Thorp (Plenum, New York, 1980); *Solid State Physics,* edited by H. Ehrenreich, F. Seitz, and D. Turnbull (Academic, New York, 1980), Vol. 35.

[7]K. K. Norskov and N. D. Lang, Phys. Rev. B **21**, 2136 (1980); M. J. Stott and E. Zaremba, *ibid.* **22**, 1564 (1980).

[8]M. Weinert and A. J. Freeman, J. Magn. Magn. Mater. **38**, 23 (1983).

[9]B. P. Feuston, R. K. Kalia, and P. Vashishta, Phys. Rev. B **35**, 6222 (1987).

[10]K. Raghavachari and V. Logovinsky, Phys. Rev. Lett. **55**, 2853 (1985).

[11]E. Blaisten-Barojas and S. N. Khanna, Phys. Rev. Lett. **61**, 1477 (1988).

[12]J. C. Slater and G. F. Koster, Phys. Rev. **94**, 1498 (1954).

[13]F. Cyrot-Lackmann, J. Phys. (Paris) **4**, 670 (1970).

[14]M. Stampanoni, A. Vaterlaus, D. Pescia, M. Aeschlimann, F. Meier, W. Durr, and S. Blugel, Phys. Rev. B **37**, 10 380 (1988); C. L. Fu, A. J. Freeman, and T. Oguchi, Phys. Rev. Lett. **54**, 2700 (1985); C. L. Fu and A. J. Freeman, J. Magn. Magn. Mater. **54-57**, 777 (1986); J. G. Gay and R. Richter, Phys. Rev. Lett. **56**, 2728 (1986); J. Appl. Phys. **61**, 3362 (1987); W. Drube and F. J. Himpsel, Phys. Rev. B **35**, 4131 (1987).

[15]S. Ohnishi, A. J. Freeman, and M. Weinert, Phys. Rev. B **28**, 6741 (1983); H. Krakauer, A. J. Freeman, and E. Wimmer, *ibid.* **28**, 610 (1983); A. J. Freeman, J. H. Xu, and T. Jarlborg, J. Magn. Magn. Mater. **31**, 909 (1983); A. J. Freeman, *ibid.* **35**, 31 (1983).

[16]O. Jepson, J. Madsen, and O. K. Anderson, Phys. Rev. B **26**, 2790 (1982).

[17]D. E. Ellis, Int. J. Quantum Chem. **S2**, 35 (1968); D. E. Ellis and G. S. Painter, Phys. Rev. B **2**, 2887 (1970).

[18]L. Hedin and B. I. Lundquist, J. Phys. C **4**, 2064 (1971); V. von Barth and L. Hedin, *ibid.* **5**, 1629 (1972).

[19]J. P. Gaspard and F. Cyrot-Lackmann, J. Phys. C **6**, 3077 (1973).

[20]D. A. Papaconstantopoulos, *Handbook of the Band Structure of Elemental Solids* (Plenum, New York, 1986).

[21]V. L. Moruzzi, J. F. Janak, and A. R. Williams, *Calculated Electronic Properties of Metals* (Pergamon, New York, 1978).

[22]D. M. Cox, D. J. Trevor, R. L. Whetter, E. A. Rohlfing, and A. Kaldos, Phys. Rev. B **32**, 7290 (1985).

[23]G. M. Pastor, J. Dorantes-Davila, and K. H. Bennemann, Physica B **149**, 22 (1988); K. Lee, J. Callaway, K. Kwong, R. Tang, and A. Ziegler, Phys. Rev. B **31**, 1796 (1985).

[24]D. J. Chadi, Phys. Rev. B **29**, 785 (1984); J. Robertson, Adv. Phys. **32**, 361 (1983).